METHOD FOR EXTENDING THE BANDWIDTH OF THE RECTANGULAR WAVEGUIDES

Valerică COSTIN[1]

In this paper is presented a method for extending the bandwidth of the rectangular waveguides. It consists of introducing the steps, with sharp edges, in the cross section of the guide, along the propagation direction.

Keywords: cutoff wavenumbers, cutoff frequencies

1. Introduction

This paper proposes a method for extending the bandwidth of rectangular waveguides. It consists of using as many steps as necessary, with sharp edges, in the cross section of the guide, along the propagation direction, together with using of local coordinates for writing the expressions of magnetic and electric components of the wave in the regions of the waveguide.

For example, the theoretical lowest cutoff frequency of a rectangular waveguide, with the cross sectional dimensions $a\times b = 29\times 13$, is $f_{c-\mathrm{TE10}} = c/2a = 5.168$ GHz. By introducing a single step in the cross section of this guide, as is shown in fig.3, the lowest cutoff frequency decreases to $f_{c-0} = 3.255$ GHz.

The coupled-integral equations technique is used, [1].

2. General theory

Fig. 1 in this paper shows a waveguide with two steps in the cross section, along the propagation direction. The edges of the steps are sharp, with the measure of internal angles of 90^0. The regions R_1, R_2, and R_3 can be distinguished in the cross section. Between the three regions there are two interfaces. The interface k is situated between regions R_k and R_{k+1}, $k = 1,\ 2$. The heights of the regions are denoted b_1, b_2, b_3. The widths of the regions are denoted l_1, l_2, l_3.

All metallic surfaces are assumed lossless in the following analysis, [1, page 2257].

The Ox axis is common for all three regions. Similarly, the propagation direction for all regions is Oz axis. For y have been used two local ordinate axes O_1y_1 and O_2y_2. They are placed within the interfaces, the origins being in the middle of the apertures.

[1] Instrument and Controls Engineer, Romania, e-mail: costin.valerica@gmail.com

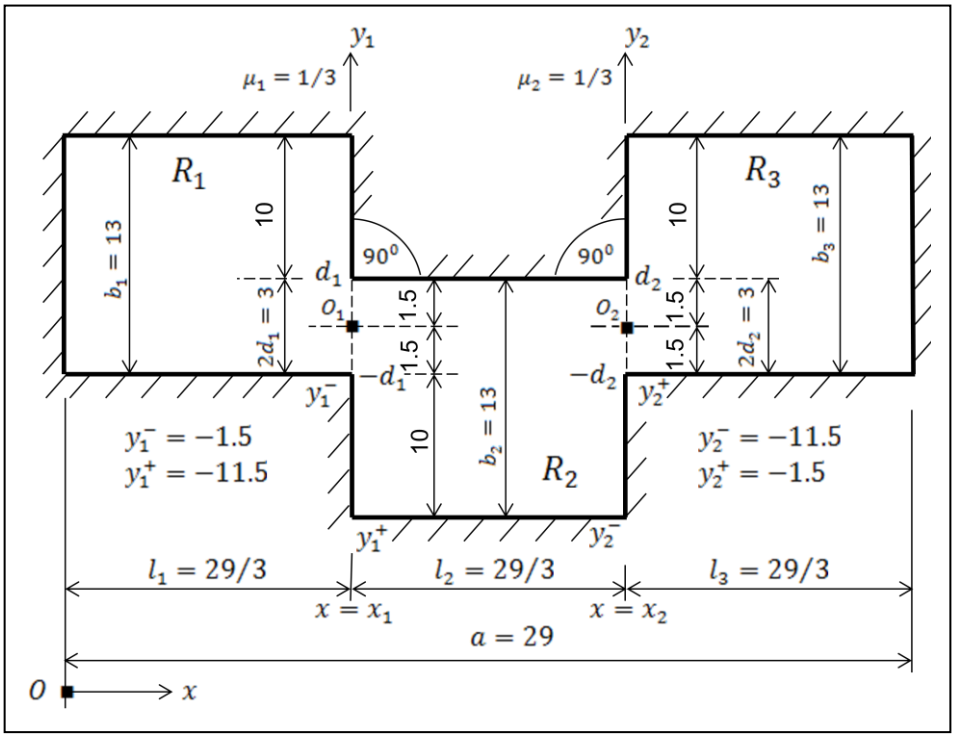

Fig. 1. Waveguide with two steps in the cross section; all dimensions are in mm; the sketch is not shown at scale.

Along the propagation direction, at $x = x_1$ and $x = x_2$, there are step discontinuities having the apertures $2d_1$ and $2d_2$.

The dimensions of the guide, together with the ordinates of the bottom walls are used in order to express the components of the wave in all the three regions. The ordinates of the bottom walls are: y_1^-, y_1^+ in O_1y_1 ordinate axes, and y_2^-, y_2^+ in O_2y_2.

2.1 Transverse Electric Modes analysis

In this paper are analyzed only Transverse Electric Modes.

2.2 Mathematically expressions of the components of the wave

The starting point for getting the expressions of axial and transverse components of the wave is the Helmholtz equations of axial components $H_z^{R_k}(x, y_k)$ in all the three regions. The boundary conditions of the problem, for all the three regions, are vanishing of the tangential electric fields in the metallic walls of the guide.

The separation of variables method is used in order to solve the problem in all the regions. In each region, the electrical components are expanded in modes

that satisfy all the boundary conditions of the region, except those in the planes of interfaces, [1, page 2257]. The results for all the regions are mentioned below:

$$H_z^{R_1}(x,y_1)=\sum_{n=0}^{\infty}A_n^{R_1}\frac{\cosh(\gamma_{1n}x)}{\cosh(\gamma_{1n}x_1)}\cos\left[\frac{n\pi}{b_1}(y_1-y_1^-)\right], \quad 0\le x\le x_1 \tag{1}$$

$$E_y^{R_1}(x,y_1)=\frac{j\omega\mu}{k_c^2}\sum_{n=0}^{\infty}A_n^{R_1}\gamma_{1n}\frac{\sinh(\gamma_{1n}x)}{\cosh(\gamma_{1n}x_1)}\cos\left[\frac{n\pi}{b_1}(y_1-y_1^-)\right], \quad 0\le x\le x_1$$

$$H_z^{R_2}(x,y_1)=\sum_{n=0}^{\infty}[A_n^{R_2}e^{\gamma_{2n}x}+B_n^{R_2}e^{-\gamma_{2n}x}]\cos\left[\frac{n\pi}{b_1}(y_1-y_1^+)\right], \quad x_1\le x\le x_2$$

$$E_y^{R_2}(x,y_1)=\frac{j\omega\mu}{k_c^2}\sum_{n=0}^{\infty}\gamma_{2n}[A_n^{R_2}e^{\gamma_{2n}x}-B_n^{R_2}e^{-\gamma_{2n}x}]\cos\left[\frac{n\pi}{b_1}(y_1-y_1^+)\right], \quad x_1\le x\le x_2$$

$$H_z^{R_2}(x,y_2)=\sum_{n=0}^{\infty}[A_n^{R_2}e^{\gamma_{2n}x}+B_n^{R_2}e^{-\gamma_{2n}x}]\cos\left[\frac{n\pi}{b_2}(y_2-y_2^-)\right], \quad x_1\le x\le x_2$$

$$E_y^{R_2}(x,y_2)=\frac{j\omega\mu}{k_c^2}\sum_{n=0}^{\infty}\gamma_{2n}[A_n^{R_2}e^{\gamma_{2n}x}-B_n^{R_2}e^{-\gamma_{2n}x}]\cos\left[\frac{n\pi}{b_2}(y_2-y_2^-)\right], \quad x_1\le x\le x_2$$

$$H_z^{R_3}(x,y_2)=\sum_{n=0}^{\infty}A_n^{R_3}\frac{\cosh(\gamma_{3n}(x-a)}{\cosh(\gamma_{3n}l_3)}\cos\left[\frac{n\pi}{b_3}(y_2-y_2^+)\right], \quad x_2\le x\le a$$

$$E_y^{R_3}(x,y_2)=\frac{j\omega\mu}{k_c^2}\sum_{n=0}^{\infty}A_n^{R_3}\gamma_{3n}\frac{\sinh(\gamma_{3n}(x-a))}{\cosh(\gamma_{3n}l_3)}\cos\left[\frac{n\pi}{b_3}(y_2-y_2^+)\right], \quad x_2\le x\le a.$$

$\gamma_{1n}^2=(n\pi/b_1)^2-k_c^2$, $\gamma_{2n}^2=(n\pi/b_2)^2-k_c^2$, $\gamma_{3n}^2=(n\pi/b_3)^2-k_c^2$.
$\gamma_{1n}, \gamma_{2n}, \gamma_{3n}$, = propagation constants of the mode n in the regions R_1, R_2, R_3.
k_c= the cutoff wavenumber of the guide.

Determining of the modal development coefficients $A_n^{R_1}$, $A_n^{R_2}$, $B_n^{R_2}$, $A_n^{R_3}$ is described in section 5.

3. Singularities of the electric fields tangent to the sharp edges

The next step is finding out of the expressions of these components in the interfaces between the regions. To do this it should be observed that the transverse electrical fields of electromagnetic wave are singular in the vicinity of the sharp vertices, [1, page 2258].

Fig. 2 shows a waveguide with metallic walls, having the cross section $a \times b$. On the upper wall there is a sharp ridge having the measure of the internal angle ϕ radians, [2, page 631].

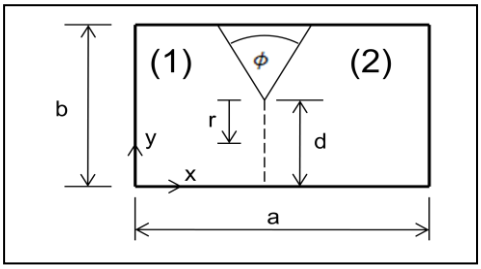

Fig. 2. Waveguide with a sharp ridge between regions (1) and (2).

The distance from the vertex of the ridge to a current point in the interface is denoted with r. The electric component of the wave, E_y, which is tangent to the interface, exhibits a singularity. According to the mentioned research works in [2, page 631], the electric field of the wave, tangent to the interface is of the form $r^{-1+\tau}$:

$$E_y(x,y) = O(r^{-1+\tau}) = O\left(r^{\nu-1/2}\right), \quad \nu = \tau - 1/2, \quad \tau = \pi/(2\pi - \phi) > 0. \tag{2}$$

For the guide in fig. 1, the internal angles of the sharp edges of the steps in the two interfaces are $\pi/2$ radians. Consequently, $E_y(x,y) = O\left(r^{\nu-1/2}\right) = O\left(r^{-1/3}\right) = O\left(1/r^{1/3}\right) = O(1/r^{\mu_k})$, where $\mu_k = 1/3$.

4. Basis and testing functions

For the guide in fig.1, the electric fields in the interfaces can be described using two sets of basis functions.

4.1 The basis functions and the functions that are describing the true distribution of the tangential electric fields in the interfaces

a) Basis functions

For the current interface, the basis functions that satisfy all edge and contour criteria, [1, page 2259], are given by the following relations:

$$X_{j,\mu_k}(y_k) = \frac{\cos[(j-1)\pi(y_k/2d_k)]}{[1-(y_k/d_k)^2]^{\mu_k}}, \qquad Y_{j,\mu_k}(y_k) = \frac{\sin[j\pi(y_k/2d_k)]}{[1-(y_k/d_k)^2]^{\mu_k}}, \qquad j = 1, 2, \dots . \tag{3}$$

In the two interfaces of the guide in fig. 1, $\mu_k = 1/3$, $k = 1, 2$.

b) The functions used for describing electrical fields in interfaces

These functions, denoted $f_1(y_1)$ and $f_2(y_2)$, are chosen such that to represent the true distribution of the electric fields in interfaces, [1, page 2257]. These functions will be zero on all metallic surfaces in interfaces and will be non

zero in the apertures of the interfaces. For the current interface, these functions are given by the expressions mentioned below in (4), [1, page 2258]:

$$f_k(y_k) = \frac{j\omega\mu}{k_c^2}\sum_{j=1}^{\infty}\left[p_{j,k}X_{j,\mu_k}(y_k) + q_{j,k}Y_{j,\mu_k}(y_k)\right], \qquad k = 1,\ 2\ , \quad j = 1, 2, \dots . \tag{4}$$

$f_k(y_k) \neq 0$ for $y_k \in (-d_k, d_k)$, $\quad f_k(y_k) = 0$ for $y_k \in [y_k^-, -d_k\ ] \cup [d_k, y_k^+ + b_{k+1}\ ]$.

where $p_{j,k}$ and $q_{j,k}$ are the series expansion coefficients, $k = 1,\ 2$.

4.2 The testing functions of the magnetic components in interfaces

The testing functions are obtained from the basis functions by simply adding $\pi/2$ to $(j-1)\pi$ or to $j\pi$ in the arguments of basis functions, because $\boldsymbol{H}$ leads $\boldsymbol{E}$ by $\pi/2$ in respect to the propagation direction. In order to be differentiated from the basis functions, the index j is replaced by i and to avoid the confusions between basis functions and testing functions, even the letters are changed, so that the following notations are used:

$$R_{i,\mu_k}(y_k) = \frac{\cos\left[\left(i-\frac{1}{2}\right)\pi(y_k/2d_k)\right]}{[1-(y_k/d_k)^2]^{\mu_k}};\ T_{i,\mu_k}(y_k) = \frac{\sin\left[\left(i+\frac{1}{2}\right)\pi(y_k/2d_k)\right]}{[1-(y_k/d_k)^2]^{\mu_k}};\ i = j = 1, 2, \dots; k = 1,\ 2. \tag{5}$$

5. Determining the modal development coefficients and the components of the Fourier spectrum for the basis and testing functions

The way to get the modal development coefficients $A_n^{R_1}$, $A_n^{R_2}$, $B_n^{R_2}$, $A_n^{R_3}$, is as follows:

a) The equality between the electrical components of the wave in the regions adjacent to current interface k and the corresponding function $f_k(y_k)$ is written, $k = 1,\ 2$;

b) The above equalities are multiplied by trigonometric functions from the orthogonal series corresponding to those of electrical components;

c) Finally, the four equalities are integrated across the apertures of the interfaces.

5.1 Determining the modal development coefficients

There will be 4 coupled-integral equations and once they are manipulated they will get different forms. For this reason, the current number of each group of equations is followed by the figures 1^-, 1^+; 2^-, 2^+. For the interface k, $k = 1,\ 2$, the upper minus sign means that the corresponding equation is written for the region in the left side of interface k, and the upper plus sign is for the equation of the region in the right side of same interface k. The equations are:

(6)

(6. 1^-)

$$\int_{-d_1}^{d_1}\left\{\sum_{n=0}^{\infty}A_n^{R_1}\gamma_{1n}\tanh(\gamma_{1n}x_1)\cos\left[\frac{n\pi}{b_1}(y_1 - y_1^-)\right]\right\}\cos\left[\frac{m\pi}{b_1}(y_1 - y_1^-)\right]dy_1 =$$
$$\int_{-d_1}^{d_1}\left\{\sum_{j=1}^{\infty}\left[p_{j,1}\frac{\cos[(j-1)\pi(y_1/2d_1)]}{[1-(y_1/d_1)^2]^{\mu_1}} + q_{j,1}\frac{\sin[j\pi(y_1/2d_1)]}{[1-(y_1/d_1)^2]^{\mu_1}}\right]\right\}\cos\left[\frac{m\pi}{b_1}(y_1 - y_1^-)\right]dy_1,$$

$$\int_{-d_1}^{d_1}\left\{\sum_{n=0}^{\infty}\gamma_{2n}\left[A_n^{R_2}e^{\gamma_{2n}x_1}-B_n^{R_2}e^{-\gamma_{2n}x_1}\right]\cos\left[\frac{n\pi}{b_2}(y_1-y_1^{+})\right]\right\}\cos\left[\frac{m\pi}{b_2}(y_1-y_1^{+})\right]dy_1=$$
$$\int_{-d_1}^{d_1}\left\{\sum_{j=1}^{\infty}\left[p_{j,1}\frac{\cos[(j-1)\pi(y_1/2d_1)]}{[1-(y_1/d_1)^2]\mu_1}+q_{j,1}\frac{\sin[j\pi(y_1/2d_1)]}{[1-(y_1/d_1)^2]\mu_1}\right]\right\}\cos\left[\frac{m\pi}{b_2}(y_1-y_1^{+})\right]dy_1, \quad (6.1^{+})$$

$$\int_{-d_2}^{d_2}\left\{\sum_{n=0}^{\infty}\gamma_{2n}\left[A_n^{R_2}e^{\gamma_{2n}x_2}-B_n^{R_2}e^{-\gamma_{2n}x_2}\right]\cos\left[\frac{n\pi}{b_2}(y_2-y_2^{-})\right]\right\}\cos\left[\frac{m\pi}{b_2}(y_2-y_2^{-})\right]dy_2=$$
$$\int_{-d_2}^{d_2}\left\{\sum_{j=1}^{\infty}\left[p_{j,2}\frac{\cos[(j-1)\pi(y_2/2d_2)]}{[1-(y_2/d_2)^2]\mu_2}+q_{j,2}\frac{\sin[j\pi(y_2/2d_2)]}{[1-(y_2/d_2)^2]\mu_2}\right]\right\}\cos\left[\frac{m\pi}{b_2}(y_2-y_2^{-})\right]dy_2, \quad (6.2^{-})$$

$$\int_{-d_2}^{d_2}\left\{\sum_{n=0}^{\infty}-A_n^{R_3}\gamma_{3n}\tanh(\gamma_{3n}l_3)\cos\left[\frac{n\pi}{b_3}(y_2-y_2^{+})\right]\right\}\cos\left[\frac{m\pi}{b_3}(y_2-y_2^{+})\right]dy_2=$$
$$\int_{-d_2}^{d_2}\left\{\sum_{j=1}^{\infty}\left[p_{j,2}\frac{\cos[(j-1)\pi(y_2/2d_2)]}{[1-(y_2/d_2)^2]\mu_2}+q_{j,2}\frac{\sin[j\pi(y_2/2d_2)]}{[1-(y_2/d_2)^2]\mu_2}\right]\right\}\cos\left[\frac{m\pi}{b_3}(y_2-y_2^{+})\right]dy_2. \quad (6.2^{+})$$

Changing the limits of integrals, from lower to upper walls of the guide, and using the relation 3.771.8, mentioned at page 442 in the reference work [4], the integrals can be calculated. Making the notations $\delta_{n0}=1$ for $n=0$, $\delta_{n0}=0$ for $n\neq 0$ and $\nu_k=(1/2)-\mu_k$, the results of the above integrals are:

(7)

$$A_n^{R_1}\gamma_{1n}\tanh(\gamma_{1n}x_1)(1+\delta_{n0})\frac{b_1}{2}=\sum_{j=1}^{\infty}p_{j,1}d_1\frac{1}{2}\sqrt{\pi}\Gamma\left(\nu_1+\frac{1}{2}\right)\cos\left(-\frac{ny_1^{-}}{b_1}\pi\right)\left[\frac{J_{\nu_1}\left[\frac{1}{2}\left(j-1+\frac{n(2d_1)}{b_1}\right)\pi\right]}{\left[\frac{1}{2}\left(j-1+\frac{n(2d_1)}{b_1}\right)\frac{\pi}{2}\right]^{\nu_1}}+\right.$$
$$\left.\frac{J_{\nu_1}\left[\frac{1}{2}\left|j-1-\frac{n(2d_1)}{b_1}\right|\pi\right]}{\left[\frac{1}{2}\left|j-1-\frac{n(2d_1)}{b_1}\right|\frac{\pi}{2}\right]^{\nu_1}}\right]+\sum_{j=1}^{\infty}q_{j,1}d_1\frac{1}{2}\sqrt{\pi}\Gamma\left(\nu_1+\frac{1}{2}\right)\sin\left(-\frac{ny_1^{-}}{b_1}\pi\right)\left[\frac{J_{\nu_1}\left[\frac{1}{2}\left(j+\frac{n(2d_1)}{b_1}\right)\pi\right]}{\left[\frac{1}{2}\left(j+\frac{n(2d_1)}{b_1}\right)\frac{\pi}{2}\right]^{\nu_1}}-\frac{J_{\nu_1}\left[\frac{1}{2}\left|j-\frac{n(2d_1)}{b_1}\right|\pi\right]}{\left[\frac{1}{2}\left|j-\frac{n(2d_1)}{b_1}\right|\frac{\pi}{2}\right]^{\nu_1}}\right], \quad (7.1^{-})$$

$$\gamma_{2n}\left[A_n^{R_2}e^{\gamma_{2n}x_1}-B_n^{R_2}e^{-\gamma_{2n}x_1}\right](1+\delta_{n0})\frac{b_2}{2}=\sum_{j=1}^{\infty}p_{j,1}d_1\frac{1}{2}\sqrt{\pi}\Gamma\left(\nu_1+\right.$$
$$\left.\frac{1}{2}\right)\cos\left(-\frac{ny_1^{+}}{b_2}\pi\right)\left[\frac{J_{\nu_1}\left[\frac{1}{2}\left(j-1+\frac{n(2d_1)}{b_2}\right)\pi\right]}{\left[\frac{1}{2}\left(j-1+\frac{n(2d_1)}{b_2}\right)\frac{\pi}{2}\right]^{\nu_1}}+\frac{J_{\nu_1}\left[\frac{1}{2}\left|j-1-\frac{n(2d_1)}{b_2}\right|\pi\right]}{\left[\frac{1}{2}\left|j-1-\frac{n(2d_1)}{b_2}\right|\frac{\pi}{2}\right]^{\nu_1}}\right]+\sum_{j=1}^{\infty}q_{j,1}d_1\frac{1}{2}\sqrt{\pi}\Gamma\left(\nu_1+\right.$$
$$\left.\frac{1}{2}\right)\sin\left(-\frac{ny_1^{+}}{b_2}\pi\right)\left[\frac{J_{\nu_1}\left[\frac{1}{2}\left(j+\frac{n(2d_1)}{b_2}\right)\pi\right]}{\left[\frac{1}{2}\left(j+\frac{n(2d_1)}{b_2}\right)\frac{\pi}{2}\right]^{\nu_1}}-\frac{J_{\nu_1}\left[\frac{1}{2}\left|j-\frac{n(2d_1)}{b_2}\right|\pi\right]}{\left[\frac{1}{2}\left|j-\frac{n(2d_1)}{b_2}\right|\frac{\pi}{2}\right]^{\nu_1}}\right], \quad (7.1^{+})$$

$$\gamma_{2n}\left[A_n^{R_2}e^{\gamma_{2n}x_2}-B_n^{R_2}e^{-\gamma_{2n}x_2}\right](1+\delta_{n0})\frac{b_2}{2}=\sum_{j=1}^{\infty}p_{j,2}d_2\frac{1}{2}\sqrt{\pi}\Gamma\left(\nu_2+\right.$$
$$\left.\frac{1}{2}\right)\cos\left(\frac{-ny_2^{-}}{b_2}\pi\right)\left[\frac{J_{\nu_2}\left[\frac{1}{2}\left(j-1+\frac{n(2d_2)}{b_2}\right)\pi\right]}{\left[\frac{1}{2}\left(j-1+\frac{n(2d_2)}{b_2}\right)\frac{\pi}{2}\right]^{\nu_2}}+\frac{J_{\nu_2}\left[\frac{1}{2}\left|j-1-\frac{n(2d_2)}{b_2}\right|\pi\right]}{\left[\frac{1}{2}\left|j-1-\frac{n(2d_2)}{b_2}\right|\frac{\pi}{2}\right]^{\nu_2}}\right]+\sum_{j=1}^{\infty}q_{j,2}d_2\frac{1}{2}\sqrt{\pi}\Gamma\left(\nu_2+\right.$$
$$\left.\frac{1}{2}\right)\sin\left(\frac{-ny_2^{-}}{b_2}\pi\right)\left[\frac{J_{\nu_2}\left[\frac{1}{2}\left(j+\frac{n(2d_2)}{b_2}\right)\pi\right]}{\left[\frac{1}{2}\left(j+\frac{n(2d_2)}{b_2}\right)\frac{\pi}{2}\right]^{\nu_2}}-\frac{J_{\nu_2}\left[\frac{1}{2}\left|j-\frac{n(2d_2)}{b_2}\right|\pi\right]}{\left[\frac{1}{2}\left|j-\frac{n(2d_2)}{b_2}\right|\frac{\pi}{2}\right]^{\nu_2}}\right], \quad (7.2^{-})$$

(7.2⁺)

$$-A_n^{R_3}\gamma_{3n}\tanh(\gamma_{3n}l_3)(1+\delta_{n0})\frac{b_3}{2}=\sum_{j=1}^{\infty}p_{j,2}d_2\frac{1}{2}\sqrt{\pi}\Gamma\left(\nu_2+\frac{1}{2}\right)\cos\left(\frac{-ny_2^+}{b_3}\pi\right)\left[\frac{J_{\nu_2}\left[\frac{1}{2}\left(j-1+\frac{n(2d_2)}{b_3}\right)\pi\right]}{\left[\frac{1}{2}\left(j-1+\frac{n(2d_2)}{b_3}\right)\frac{\pi}{2}\right]^{\nu_2}}+\right.$$

$$\left.\frac{J_{\nu_2}\left[\frac{1}{2}\left|j-1-\frac{n(2d_2)}{b_3}\right|\pi\right]}{\left[\frac{1}{2}\left|j-1-\frac{n(2d_2)}{b_3}\right|\frac{\pi}{2}\right]^{\nu_2}}\right]+\sum_{j=1}^{\infty}q_{j,2}d_2\frac{1}{2}\sqrt{\pi}\Gamma\left(\nu_2+\frac{1}{2}\right)\sin\left(\frac{-ny_2^+}{b_3}\pi\right)\left[\frac{J_{\nu_2}\left[\frac{1}{2}\left(j+\frac{n(2d_2)}{b_3}\right)\pi\right]}{\left[\frac{1}{2}\left(j+\frac{n(2d_2)}{b_3}\right)\frac{\pi}{2}\right]^{\nu_2}}-\frac{J_{\nu_2}\left[\frac{1}{2}\left|j-\frac{n(2d_2)}{b_3}\right|\pi\right]}{\left[\frac{1}{2}\left|j-\frac{n(2d_2)}{b_3}\right|\frac{\pi}{2}\right]^{\nu_2}}\right].$$

where J_{ν_k} are Bessel functions of the first kind of order ν_k, and Γ is function gamma.

In [1, page 2261] is proved that only "two basis functions are sufficient". Because in this paper have been used the same basis functions as in [1], it is also used the same numbers of terms for j, that is $j=1,\ 2$, and of course $i=1,\ 2$.

5.2 The Fourier spectrum of the basis functions, mode n

Two notations will be done in each equation of group (7). These notations represent *the components of the Fourier spectrum of the basis functions* $X_{j,\mu_k}(y_k)$ *and* $Y_{j,\mu_k}(y_k)$, *for the mode* n, in the regions R_k and R_{k+1}, regions adjacent to the interface k, $k=1,\ 2$, [1, page 2259].

The components of the Fourier spectrum are: $\tilde{X}_{j,\mu_1}^{R_1}(n)$, $\tilde{Y}_{j,\mu_1}^{R_1}(n)$, $\tilde{X}_{j,\mu_1}^{R_2}(n)$, $\tilde{Y}_{j,\mu_1}^{R_2}(n)$, $\tilde{X}_{j,\mu_2}^{R_2}(n)$, $\tilde{Y}_{j,\mu_2}^{R_2}(n)$, $\tilde{X}_{j,\mu_2}^{R_3}(n)$ and $\tilde{Y}_{j,\mu_2}^{R_3}(n)$.

Below are presented only the expressions of the components of the Fourier spectrum, mode n, for the region R_2, written in the system O_2y_2:

$$\tilde{X}_{j,\mu_2}^{R_2}(n)=\frac{(2d_2/b_2)}{(1+\delta_{n0})}\frac{1}{2}\sqrt{\pi}\Gamma\left(\nu_2+\frac{1}{2}\right)\cos\left(-\frac{ny_2^-}{b_2}\pi\right)\left[\frac{J_{\nu_2}\left[\frac{1}{2}\left(j-1+\frac{n(2d_2)}{b_2}\right)\pi\right]}{\left[\frac{1}{2}\left(j-1+\frac{n(2d_2)}{b_2}\right)\frac{\pi}{2}\right]^{\nu_2}}+\frac{J_{\nu_2}\left[\frac{1}{2}\left|j-1-\frac{n(2d_2)}{b_2}\right|\pi\right]}{\left[\frac{1}{2}\left|j-1-\frac{n(2d_2)}{b_2}\right|\frac{\pi}{2}\right]^{\nu_2}}\right],$$

$$\tilde{Y}_{j,\mu_2}^{R_2}(n)=\frac{(2d_2/b_2)}{(1+\delta_{n0})}\frac{1}{2}\sqrt{\pi}\Gamma\left(\nu_2+\frac{1}{2}\right)\sin\left(-\frac{ny_2^-}{b_2}\pi\right)\left[\frac{J_{\nu_2}\left[\frac{1}{2}\left(j+\frac{n(2d_2)}{b_2}\right)\pi\right]}{\left[\frac{1}{2}\left(j+\frac{n(2d_2)}{b_2}\right)\frac{\pi}{2}\right]^{\nu_2}}-\frac{J_{\nu_2}\left[\frac{1}{2}\left|j-\frac{n(2d_2)}{b_2}\right|\pi\right]}{\left[\frac{1}{2}\left|j-\frac{n(2d_2)}{b_2}\right|\frac{\pi}{2}\right]^{\nu_2}}\right].$$

Introducing these notations in the group (7) of equations, the development coefficients $A_n^{R_1}$, $A_n^{R_2}$, $B_n^{R_2}$, $A_n^{R_3}$ can be obtained.

5.3 The Fourier spectrum for the testing functions, mode n

According to the section 4.2 and to the relations (5), the components of the Fourier spectrum for the testing functions, mode n, can determined, by adding $1/2$ to $(j-1)$ and to j in the components of Fourier spectrum of basis functions. These components are: $\tilde{R}_{i,\mu_1}^{R_1}(n)$, $\tilde{T}_{i,\mu_1}^{R_1}(n)$, $\tilde{R}_{i,\mu_1}^{R_2}(n)$, $\tilde{T}_{i,\mu_1}^{R_2}(n)$, $\tilde{R}_{i,\mu_2}^{R_2}(n)$, $\tilde{T}_{i,\mu_2}^{R_2}(n)$, $\tilde{R}_{i,\mu_2}^{R_3}(n)$, and $\tilde{T}_{i,\mu_2}^{R_3}(n)$.

6. The fundamental equations of the guide

The procedure for getting the fundamental equations of the guide in fig. 1 is:

a) The equality between the magnetic components of the wave in the interfaces is written, that is $H_z^{R_k}(x=x_k,y_k)=H_z^{R_{k+1}}(x=x_k,y_k)$, $k=1,\ 2$;

b) The above groups of equalities are successively multiplied by the testing functions $R_{i,\mu_k}(y_k)$ and $T_{i,\mu_k}(y_k)$ and then integrated across the apertures of interfaces.

The four equations, which are obtained, are mentioned below:

(8)

(8.1R)

$$\sum_{j=1}^{2} p_{j,1} \sum_{n=0}^{\infty}(1+\delta_{n0})\left[b_1 \frac{\tilde{X}_{j,\mu_1}^{R_1}(n)\tilde{R}_{i,\mu_1}^{R_1}(n)}{\gamma_{1n}\tanh(\gamma_{1n}l_1)} + b_2 \frac{\tilde{X}_{j,\mu_1}^{R_2}(n)\tilde{R}_{i,\mu_1}^{R_2}(n)}{\gamma_{2n}\tanh(\gamma_{2n}l_2)}\right] + \sum_{j=1}^{2} q_{j,1} \sum_{n=0}^{\infty}(1+\delta_{n0})\left[b_1 \frac{\tilde{Y}_{j,\mu_1}^{R_1}(n)\tilde{R}_{i,\mu_1}^{R_1}(n)}{\gamma_{1n}\tanh(\gamma_{1n}l_1)} + b_2 \frac{\tilde{Y}_{j,\mu_1}^{R_2}(n)\tilde{R}_{i,\mu_1}^{R_2}(n)}{\gamma_{2n}\tanh(\gamma_{2n}l_2)}\right] + \sum_{j=1}^{2} p_{j,2} \sum_{n=0}^{\infty}(1+\delta_{n0})\left[-b_2 \frac{\tilde{X}_{j,\mu_2}^{R_2}(n)\tilde{R}_{i,\mu_1}^{R_2}(n)}{\gamma_{2n}\sinh(\gamma_{2n}l_2)}\right] + \sum_{j=1}^{2} q_{j,2} \sum_{n=0}^{\infty}(1+\delta_{n0})\left[-b_2 \frac{\tilde{Y}_{j,\mu_2}^{R_2}(n)\tilde{R}_{i,\mu_1}^{R_2}(n)}{\gamma_{2n}\sinh(\gamma_{2n}l_2)}\right] = 0,$$

(8.1T)

$$\sum_{j=1}^{2} p_{j,1} \sum_{n=0}^{\infty}(1+\delta_{n0})\left[b_1 \frac{\tilde{X}_{j,\mu_1}^{R_1}(n)\tilde{T}_{i,\mu_1}^{R_1}(n)}{\gamma_{1n}\tanh(\gamma_{1n}l_1)} + b_2 \frac{\tilde{X}_{j,\mu_1}^{R_2}(n)\tilde{T}_{i,\mu_1}^{R_2}(n)}{\gamma_{2n}\tanh(\gamma_{2n}l_2)}\right] + \sum_{j=1}^{2} q_{j,1} \sum_{n=0}^{\infty}(1+\delta_{n0})\left[b_1 \frac{\tilde{Y}_{j,\mu_1}^{R_1}(n)\tilde{T}_{i,\mu_1}^{R_1}(n)}{\gamma_{1n}\tanh(\gamma_{1n}l_1)} + b_2 \frac{\tilde{Y}_{j,\mu_1}^{R_2}(n)\tilde{T}_{i,\mu_1}^{R_2}(n)}{\gamma_{2n}\tanh(\gamma_{2n}l_2)}\right] + \sum_{j=1}^{2} p_{j,2} \sum_{n=0}^{\infty}(1+\delta_{n0})\left[-b_2 \frac{\tilde{X}_{j,\mu_2}^{R_2}(n)\tilde{T}_{i,\mu_1}^{R_2}(n)}{\gamma_{2n}\sinh(\gamma_{2n}l_2)}\right] + \sum_{j=1}^{2} q_{j,2} \sum_{n=0}^{\infty}(1+\delta_{n0})\left[-b_2 \frac{\tilde{Y}_{j,\mu_2}^{R_2}(n)\tilde{T}_{i,\mu_1}^{R_2}(n)}{\gamma_{2n}\sinh(\gamma_{2n}l_2)}\right] = 0,$$

(8.2R)

$$\sum_{j=1}^{2} p_{j,1} \sum_{n=0}^{\infty}(1+\delta_{n0})\left[-b_2 \frac{\tilde{X}_{j,\mu_1}^{R_2}(n)\tilde{R}_{i,\mu_2}^{R_2}(n)}{\gamma_{2n}\sinh(\gamma_{2n}l_2)}\right] + \sum_{j=1}^{2} q_{j,1} \sum_{n=0}^{\infty}(1+\delta_{n0})\left[-b_2 \frac{\tilde{Y}_{j,\mu_1}^{R_2}(n)\tilde{R}_{i,\mu_2}^{R_2}(n)}{\gamma_{2n}\sinh(\gamma_{2n}l_2)}\right] + \sum_{j=1}^{2} p_{j,2} \sum_{n=0}^{\infty}(1+\delta_{n0})\left[b_2 \frac{\tilde{X}_{j,\mu_2}^{R_2}(n)\tilde{R}_{i,\mu_2}^{R_2}(n)}{\gamma_{2n}\tanh(\gamma_{2n}2)} + b_3 \frac{\tilde{X}_{j,\mu_2}^{R_3}(n)\tilde{R}_{i,\mu_2}^{R_3}(n)}{\gamma_{3n}\tanh(\gamma_{3n}l_3)}\right] + \sum_{j=1}^{2} q_{j,2} \sum_{n=0}^{\infty}(1+\delta_{n0})\left[b_2 \frac{\tilde{Y}_{j,\mu_2}^{R_2}(n)\tilde{R}_{i,\mu_2}^{R_2}(n)}{\gamma_{2n}\tanh(\gamma_{2n}l_2)} + b_3 \frac{\tilde{Y}_{j,\mu_2}^{R_3}(n)\tilde{R}_{i,\mu_2}^{R_3}(n)}{\gamma_{3n}\tanh(\gamma_{3n}l_3)}\right] = 0$$

(8.2T)

$$\sum_{j=1}^{2} p_{j,1} \sum_{n=0}^{\infty}(1+\delta_{n0})\left[-b_2 \frac{\tilde{X}_{j,\mu_1}^{R_2}(n)\tilde{R}_{i,\mu_2}^{R_2}(n)}{\gamma_{2n}\sinh(\gamma_{2n}l_2)}\right] + \sum_{j=1}^{2} q_{j,1} \sum_{n=0}^{\infty}(1+\delta_{n0})\left[-b_2 \frac{\tilde{Y}_{j,\mu_1}^{R_2}(n)\tilde{R}_{i,\mu_2}^{R_2}(n)}{\gamma_{2n}\sinh(\gamma_{2n}l_2)}\right] + \sum_{j=1}^{2} p_{j,2} \sum_{n=0}^{\infty}(1+\delta_{n0})\left[b_2 \frac{\tilde{X}_{j,\mu_2}^{R_2}(n)\tilde{R}_{i,\mu_2}^{R_2}(n)}{\gamma_{2n}\tanh(\gamma_{2n}2)} + b_3 \frac{\tilde{X}_{j,\mu_2}^{R_3}(n)\tilde{R}_{i,\mu_2}^{R_3}(n)}{\gamma_{3n}\tanh(\gamma_{3n}l_3)}\right] + \sum_{j=1}^{2} q_{j,2} \sum_{n=0}^{\infty}(1+\delta_{n0})\left[b_2 \frac{\tilde{Y}_{j,\mu_2}^{R_2}(n)\tilde{R}_{i,\mu_2}^{R_2}(n)}{\gamma_{2n}\tanh(\gamma_{2n}l_2)} + b_3 \frac{\tilde{Y}_{j,\mu_2}^{R_3}(n)\tilde{R}_{i,\mu_2}^{R_3}(n)}{\gamma_{3n}\tanh(\gamma_{3n}l_3)}\right] = 0$$

The letters R and T in the equations of the group (8) come from the fact the equalities between the magnetic components of the wave in the interfaces are multiplied successively by $R_{i,\mu_k}(y_k)$ and $T_{i,\mu_k}(y_k)$.

Making suitable notations in the equations of the group (8), the system of equations (9) will be obtained, where $i = j = 1,\ 2$. That system of equations is:

(9)

$$\sum_{j=1}^{2}\{p_{j,1}[U1]_{ij} + q_{j,1}[V1]_{ij} + p_{j,2}[W1]_{ij} + q_{j,2}[X1]_{ij}\} = 0,$$

$$\sum_{j=1}^{2}\{p_{j,1}[U2]_{ij} + q_{j,1}[V2]_{ij} + p_{j,2}[W2]_{ij} + q_{j,2}[X2]_{ij}\} = 0,$$
$$\sum_{j=1}^{2}\{p_{j,1}[U3]_{ij} + q_{j,1}[V3]_{ij} + p_{j,2}[W3]_{ij} + q_{j,2}[X3]_{ij}\} = 0,$$
$$\sum_{j=1}^{2}\{p_{j,1}[U4]_{ij} + q_{j,1}[V4]_{ij} + p_{j,2}[W4]_{ij} + q_{j,2}[X4]_{ij}\} = 0,$$

The cutoff wavenumbers of the TE modes are determined as the zeros of the determinant of the matrix in the system of equations (9), [1, page 2258]. "It is numerically more advantageous to locate the zero of the smallest singular value instead, as this allows the suppression of the poles that are otherwise present in the determinant", [1, page 2258]. Getting the smallest singular value is described in [3].

7. Numerical results

The determinant $D(k)$ of the matrix in the system (9) of equations is graphically represented as a function of the wave numbers k, in the range 0 to 1 rad/mm. The intersections of the graph with "Ok" axis represent the cutoff wavenumbers of the guide. Doing so, for the lowest cutoff wavenumber of the guide in fig. 1 has been obtained the value $k_{c-0} = 0.06284$ rad/mm and, for the corresponding lowest cutoff frequency has been obtained the value $f_{c-0} = 2.998$ GHz.

8. Extending the bandwidth

The theoretical lowest cutoff frequency of a rectangular waveguide with the cross sectional dimensions $a{\times}b = 29{\times}13$ is $f_{c-\mathrm{TE10}} = c/2a = 5.168$ GHz. Introducing two steps in the cross section of this guide, but maintaining the same height of 13 mm in all the three regions and the same total internal width of 29 mm, the guide in fig. 1 has been obtained. For this guide, has been shown in section (7) that the lowest cutoff frequency has been decreased to $f_{c-0} = 2.998$GHz, proving that the bandwidth has been extended.

9. Validating the method

Using the local coordinates, the method presented above has been applied to the guide analyzed in reference work [1, page 2257], even though that guide is a ridged one. The data in the work [1, page 2262] have been compared to the data obtained using the method exposed above. The results can be seen in the table 1.

Table 1.

The cutoff wavenumbers in the table are measured in rad/mm.

	Mode	0	1	2	3	4
Present method	k_c	0.09299	0.32971	0.33316	0.33518	0.38115
[1,pag.2262]	k_c	0.0926		0.3332		0.3811
	Mode	5	6	7	8	9
Present method	k_c	0.46904	0.52666	0.66527	0.69123	0.74546

[1,pag.2262]	k_c		0.5263	0.6653	0.6916	0.7453
	Mode	10	11	12	13	14
Present method	k_c	0.74653	0.83028	0.93941	0.96122	0.99690
[1,pag.2262]	k_c		0.8295			

The data seem to be very close. It can be seen that in this paper have been used 5 significant digits after the decimal point.

10. The importance of the method

The waveguides with the cross sections in steps are more easily to be manufactured than the ridged waveguides. For example, the width of the ridge of the waveguide analyzed in [1] is of only 0.3 mm, which is very difficult to be obtained.

The method can be used in order to design guiding structures with the desired bandwidth, acting upon the number of the steps, upon their locations in the cross section and upon the magnitude of apertures. For example, in fig. 3 is shown a waveguide with the same overall dimensions $a \times b = 29 \times 13$, like the guide in fig. 1 but, with a single step placed at the middle of the cross section. The aperture of the guide in fig. 3 is of 3 mm, like the apertures of the guide in fig.1.

The lowest cutoff wavenumber of the guide in fig. 3 is $k_{c-0} = 0.06823$ rad/mm and the corresponding lowest cutoff frequency is $f_{c-0} = 3.255$ GHz.

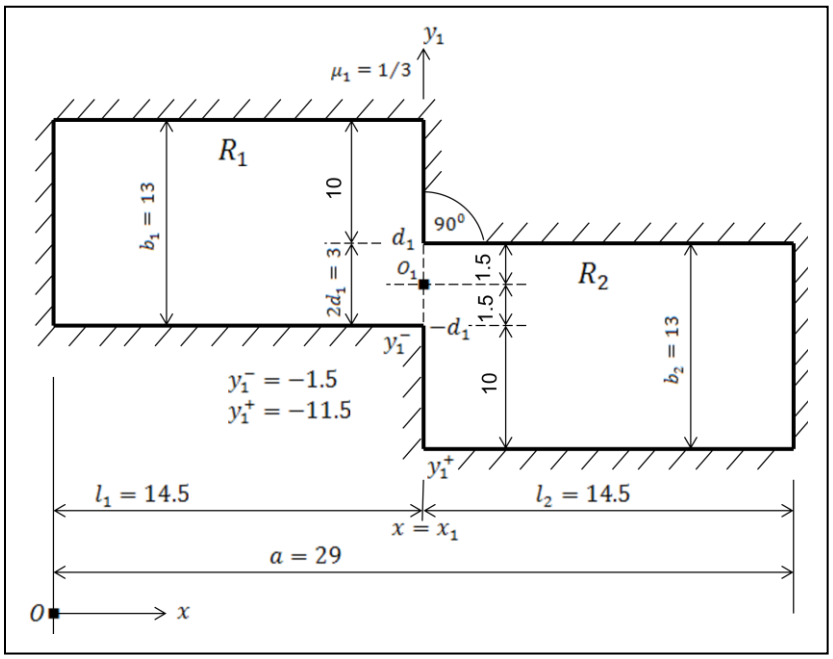

Fig. 3. Wave guide with a single step in the cross section;

$$k_{c-0} = 0.06823,\ f_{c-0} = 3.255 \text{ GHz}.$$

The steps can be located anywhere in the cross section of the guide, $l_1 \neq l_2 \neq \cdots \neq l_n$, so that the guides without any symmetry can be analyzed. For example, if in fig. 1, the widths of the regions l_1, l_2, l_3, the aperture $2d_2$ and the ordinate y_2^+ are modified to the values $l_1 = 8$, $l_2 = 12$, $l_3 = 9$, $2d_3 = 4.5$ and $y_2^+ = -2.25$, while the heights of the three regions are kept at 13 mm than, the lowest cutoff frequency of that guide becomes $f_{c-0} = 3.277$ GHz.

The number of the steps in the cross section of a guide can be increased as much as necessary, in order to obtain the desired bandwidth. However, increasing the number of steps does not guarantee a lower cutoff wavenumber.

R E F E R E N C E S

[1]. *Smain Amari, Jenes Bornemann, Ruediger Vahldieck*, "Application of Coupled-Integral-Equations Technique to Ridged Waveguides", IEEE Transactions on Microwave Theory and Techniques, vol.44, No.12, pp. 2256-2263, December 1996.

[2]. *Dorel Homentcovschi and Ronald N. Miles*, "A re-expansion method for determining the acoustical impedance and the scattering matrix for the waveguide discontinuity problem", J. Acoustic Soc. Am. 128 _2_, August 2010, pages 628-638.

[3]. *Vladimir A. Labay and Jens Bornemann*, "Matrix Singular Value Decomposition for Pole-Free Solutions of Homogeneous Matrix Equations as Applied to Numerical Modeling Methods", IEEE microwave and Guided Wave letters, vol.2, no.2, February 1992.

[4]. *I.S.Gradsteyn, I. M. Ryhzik*, "Table of integrals, series and products", seventh edition.

[5]. *Ivica Stevanovic, Pedro Crespo-Valero and Juan R. Mosig*, "An Integral-Equation Technique for Solving Thick Irises in Rectangular Waveguides", IEEE Transactions on Microwave Theory and Techniques, Vol. 54, No. 1, January 2006.

[6]. *Dorel Homentcovschi and Ronald N. Miles*, "Re-expansion method for circular waveguide discontinuities: Application to concentric expansion chambers", J. Acoustic Soc. Am., Vol. 131, No. 2, February 2012.

[7]. *Alvin Wexler*, "Solution of Waveguide Discontinuities by Modal Analysis", IEEE Transactions on Microwave Theory and Techniques, Vol. MTT-15, No. 9, September 1967.

[8]. *Smain Amari, Jenes Bornemann, Ruediger Vahldieck*, "Fast and Accurate Analysis of Waveguide Filters by the Coupled-Integral-Equations- Technique", IEEE Transactions on Microwave Theory and Techniques, Vol. 45, No. 9, September 1997.

[9]. Z. *Hradecký, M. Mazánek*, "Nonstandard Double Ridged Waveguide Mode Study", Czech Technical University in Prague, Department of Electromagnetic Field, Technická 2, 166 27 Prague 6, Czech Republic.

[10]. *Dorel Homentcovschi, Anton Manolescu, Anca Manuela Manolescu and Liviu Kreindler, "*An Analytical Solution for the Coupled Stripline-Like Microstrip Line Problem", IEEE Transactions on Microwave Theory and Techniques, Vol.36, No.6, June 1988.

[11]. *Dorel Homentcovschi and Radu Oprea*, "Analytically Determined Quasi-Static Parameters of Shielded or Open Multiconductor Microstrip Lines", IEEE Transactions on Microwave Theory and Techniques, Vol. 46, No.1, January 1998.

[12]. *Dorel Homentcovschi*, „**A** Cylindrical Multiconductor Stripline-Like Microstrip Transmission Line", IEEE Transactions on Microwave Theory and Techniques, Vol. 37, No. 3, March 1989.